Secondary instability in boundarylayer flows

Ali H. Nayfeh and Ali N. Bozatli

Citation: Physics of Fluids (1958-1988) **22**, 805 (1979); doi: 10.1063/1.862680
View online: http://dx.doi.org/10.1063/1.862680
View Table of Contents: http://scitation.aip.org/content/aip/journal/pof1/22/5?ver=pdfcov
Published by the AIP Publishing

Secondary instability in boundary-layer flows

Ali H. Nayfeh and Ali N. Bozatli

Department of Engineering Science and Mechanics, Virginia Polytechnic Institute and State University, Blacksburg, Virginia 24061
(Received 19 June 1978; final manuscript received 15 January 1979)

The stability of a secondary Tollmien–Schlichting wave, whose wavenumber and frequency are nearly one half those of a fundamental Tollmien–Schlichting instability wave, is analyzed using the method of multiple scales. Under these conditions, the fundamental wave acts as a parametric exciter for the secondary wave. The results show that the amplitude of the fundamental wave must exceed a critical value to trigger this parametric instability. This value is proportional to a detuning parameter which is the real part of $k - 2K$, where k and K are the wavenumbers of the fundamental and its subharmonic, respectively. For Blasius flow, the critical amplitude is approximately 29% of the mean flow, and hence many other secondary instabilities take place before this parametric instability becomes significant. For other flows where the detuning parameter is small, such as free-shear layer flows, the critical amplitude can be small, thus the parametric instability might play a greater role.

I. INTRODUCTION

One of the major roads from laminar to turbulent conditions in two-dimensional boundary-layer flows starts with the linear amplification of selective two-dimensional disturbances of the Tollmien–Schlichting type. As these disturbances grow to appreciable magnitudes, the flow deviates more and more from a basic steady flow, and as a result, secondary instabilities set in. Klebanoff *et al.*,[1] in their experimental study of the three-dimensional nature of boundary-layer instability, observed secondary instabilities induced by the nonlinear interaction between a two-dimensional fundamental wave and a three-dimensional secondary wave at a position not very far from the linear region. Kachanov *et al.*[2] excited disturbances of known frequencies on a flat plate using a vibrating ribbon and determined the spectrum of the disturbances at different downstream locations. Their results show that the higher harmonics and subharmonics of the fundamental wave start to amplify faster than the fundamental wave itself. These results were also confirmed in Ref. 3.

In his experiments on the natural transition from laminar to turbulent flow in a two-dimensional separated shear layer, Sato[4] observed the strong presence of the subharmonic of order one-half in addition to the higher harmonics of the fundamental wave. Wille[5] observed the development of subharmonic waves while investigating circular and plane jets. Kelly[6] analyzed the interactions among disturbance waves in an inviscid shear layer with a hyperbolic tangent velocity profile to model the observed behavior of the subharmonic waves in the free-shear layer experiments. He showed that the appearance of the subharmonic in a shear layer is due to a secondary linear instability associated with a time-dependent flow consisting of the superposition of the basic flow and a finite-amplitude fundamental wave. He concluded that the subharmonic wave not only appears in the disturbance spectrum of the flow, but that it may also grow more than the fundamental wave when the amplitude of the latter reaches a critical value. Thus, the fundamental wave serves as a means by which further energy is transferred from the mean flow to the subharmonic wave.

The purpose of the present paper is to investigate whether one of these secondary instabilities can explain the appearance of the subharmonic wave on a flat plate. The analysis takes into account the growth of the mean boundary layer as well as the effects of viscosity in the disturbance equations.

To analyze the secondary instability of order one-half in a nonparallel boundary layer, we first need to determine the mean flow and the nonparallel growth of the fundamental wave. The mean flow is given by the Blasius solution

$$u = U_0(\epsilon_1 x, y), \quad v = \epsilon_1 V_0(\epsilon_1 x, y), \quad p = P_0, \tag{1}$$

where u and v are the streamwise and transverse components of the velocity and p is the pressure. Here, ϵ_1 is a small dimensionless parameter that is a measure of the nonparallelism of the flow. Using the method of multiple scales,[7] we can approximate the nonparallel linear Tollmien–Schlichting waves by[8,9]

$$u = \epsilon A(\epsilon_1 x) U_1(\epsilon_1 x, y) \exp[i \int k(\epsilon_1 x) dx - i\omega t] + \text{c.c.}, \tag{2}$$

$$v = \epsilon A(\epsilon_1 x) V_1(\epsilon_1 x, y) \exp[i \int k(\epsilon_1 x) dx - i\omega t] + \text{c.c.}, \tag{3}$$

$$p = \epsilon A(\epsilon_1 x) P_1(\epsilon_1 x, y) \exp[i \int k(\epsilon_1 x) dx - i\omega t] + \text{c.c.}, \tag{4}$$

where ϵ is a small dimensionless parameter that is the order of the amplitude of the wave and

$$f_1(\epsilon_1 x)(dA/dx) = \epsilon_1 f_3(\epsilon_1 x) A, \tag{5}$$

with f_1 and f_3 being known functions of the eigenvalue, the eigenfunction and its adjoint, and the mean flow. In all the numerical calculations presented in this paper, ϵ is taken to be the initial amplitude of the fundamental wave as a fraction of the mean flow.

In analyzing the generation of the subharmonic of order one-half, we take into account the nonparallel effects that arise from the growth of the boundary layer, which is characterized by ϵ_1, as well as the presence of the fundamental wave, which is characterized by ϵ. When $\epsilon_1 \ll \epsilon$, the effect of the boundary-layer growth is negligible in comparison with the secondary instability.

 0031-9171/79/050805-09$00.90

When $\epsilon_1 \gg \epsilon$, the effect of the secondary instability is negligible in comparison with the effect of the boundary-layer growth. When $\epsilon = O(\epsilon_1)$, both effects are comparable and this is the case treated in this paper. However, since the algebra is quite involved for this general case, we present the details of the analysis for the case $\epsilon_1 \ll \epsilon$ (i.e., parallel mean flow) and just state the results in Sec. IV for the general case.

The formulation of the problem is given in Sec. II, the solution for the problem of secondary instability is given in Sec. III, the equations describing the general problem are stated in Sec. IV, the computational procedure is described in Sec. V, and the numerical results are presented in Sec. VI.

II. PROBLEM FORMULATION

We consider secondary instabilities of a two-dimensional, steady, incompressible flow past a flat plate. The equations describing the motion are the unsteady, dimensionless Navier–Stokes equations

$$\frac{\partial U}{\partial x} + \frac{\partial V}{\partial y} = 0 , \tag{6}$$

$$\frac{\partial U}{\partial t} + U\frac{\partial U}{\partial x} + V\frac{\partial U}{\partial y} = -\frac{\partial P}{\partial x} + \frac{1}{R}\nabla^2 U , \tag{7}$$

$$\frac{\partial V}{\partial t} + U\frac{\partial V}{\partial x} + V\frac{\partial V}{\partial y} = -\frac{\partial P}{\partial y} + \frac{1}{R}\nabla^2 V , \tag{8}$$

$$U = V = 0, \quad \text{at } y = 0 , \tag{9}$$

$$U \to U_\infty, \quad \text{as } y \to \infty , \tag{10}$$

where

$$\nabla^2 = \frac{\partial^2}{\partial x^2} + \frac{\partial^2}{\partial y^2} .$$

Here, x and y are made dimensionless by using a reference length δ_r, the time is made dimensionless by using δ_r/U_∞, the velocities are made dimensionless by using the freestream velocity U_∞, and the pressure is made dimensionless by using ρU_∞^2. The Reynolds number is defined as $R = U_\infty \delta_r/\nu$, where ν is the fluid kinematic viscosity. In all the calculations presented in this paper, $\delta_r = (\nu x/U_\infty)^{1/2}$ so that $R = (R_x)^{1/2}$.

A. Basic state

As mentioned in the introduction, we present the details of the analysis for the case of a parallel mean flow. We assume that each basic-flow quantity is the sum of a mean-flow quantity and an unsteady disturbance quantity made up from a Tollmien–Schlichting wave; that is,

$$\hat{U}(x,y,t) = U_0(y) + \epsilon U_1(y)\exp[i(kx - \omega t)] + \text{c.c.} + O(\epsilon^2) , \tag{11}$$

$$\hat{V}(x,y,t) = \epsilon V_1(y)\exp[i(kx - \omega t)] + \text{c.c.} + O(\epsilon^2) , \tag{12}$$

$$\hat{P}(x,y,t) = P_0 + \epsilon P_1(y)\exp[i(kx - \omega t)] + \text{c.c.} + O(\epsilon^2) , \tag{13}$$

where U_0 and P_0 are the mean-flow quantities, ϵ is the amplitude of the Tollmien–Schlichting wave, and c.c. stands for the complex conjugate of the preceding terms. The dimensionless angular frequency is represented by ω and the real part of k is the wavenumber whereas the imaginary part of k is the negative of the growth rate. von Kerczek[10] treated the case for which Eqs. (11)–(13) are independent of x.

Substituting Eqs. (11)–(13) into Eqs. (6)–(8), subtracting the mean-flow quantities, and linearizing the resulting equations in the unsteady disturbance quantities, we obtain the following equations describing the Tollmien–Schlichting wave:

$$\mathfrak{L}_1(U_1, V_1; k) \equiv DV_1 + ikU_1 = 0 , \tag{14}$$

$$\mathfrak{L}_2(U_1, V_1, P_1; k, \omega) \equiv i(U_0 k - \omega)U_1 + V_1 DU_0 + ikP_1 - R^{-1}(D^2 - k^2)U_1 = 0 , \tag{15}$$

$$\mathfrak{L}_3(U_1, V_1, P_1; k, \omega) \equiv i(U_0 k - \omega)V_1 + DP_1 - R^{-1}(D^2 - k^2)V_1 = 0 , \tag{16}$$

$$U_1 = V_1 = 0, \quad \text{at } y = 0 , \tag{17}$$

$$U_1, V_1 \to 0, \quad \text{as } y \to \infty , \tag{18}$$

where $D \equiv \partial/\partial y$.

B. Stability analysis

To study the stability of the basic state, we superpose small unsteady disturbances on the basic-flow quantities according to

$$U(x,y,t) = \hat{U}(x,y,t) + \tilde{u}(x,y,t) , \tag{19}$$

$$V(x,y,t) = \hat{V}(x,y,t) + \tilde{v}(x,y,t) , \tag{20}$$

$$P(x,y,t) = \hat{P}(x,y,t) + \tilde{p}(x,y,t) , \tag{21}$$

where $\hat{U}$, $\hat{V}$, and $\hat{P}$ represent the basic state given by Eqs. (11)–(13) and $\tilde{u}$, $\tilde{v}$, and $\tilde{p}$ are the time dependent disturbances which are assumed to be small compared with the basic-state quantities.

Substituting Eqs. (19)–(21) into Eqs. (6)–(10), subtracting the basic-state quantities, and linearizing the resulting equations in the unsteady disturbance quantities, we obtain

$$\frac{\partial \tilde{u}}{\partial x} + \frac{\partial \tilde{v}}{\partial y} = 0 , \tag{22}$$

$$\frac{\partial \tilde{u}}{\partial t} + \hat{U}\frac{\partial \tilde{u}}{\partial x} + \tilde{u}\frac{\partial \hat{U}}{\partial x} + \hat{V}\frac{\partial \tilde{u}}{\partial y} + \tilde{v}\frac{\partial \hat{U}}{\partial y} + \frac{\partial \tilde{p}}{\partial x} - \frac{1}{R}\nabla^2\tilde{u} = 0 , \tag{23}$$

$$\frac{\partial \tilde{v}}{\partial t} + \hat{U}\frac{\partial \tilde{v}}{\partial x} + \tilde{u}\frac{\partial \hat{V}}{\partial x} + \hat{V}\frac{\partial \tilde{v}}{\partial y} + \tilde{v}\frac{\partial \hat{V}}{\partial y} + \frac{\partial \tilde{p}}{\partial y} - \frac{1}{R}\nabla^2\tilde{v} = 0 , \tag{24}$$

$$\tilde{u} = \tilde{v} = 0, \quad \text{at } y = 0 , \tag{25}$$

$$\tilde{u}, \tilde{v} \to 0, \quad \text{as } y \to \infty . \tag{26}$$

Thus, the problem of secondary instability is reduced to the analysis of the partial differential equations (22)–(24) subject to the boundary conditions (25) and (26). The coefficients in these equations are functions of x, y, and t. If $\epsilon \ll 1$, the variations in x and t, which are periodic, are small. When $\epsilon = 0$, one of the solutions

of Eqs. (22)–(26) is a Tollmien–Schlichting wave of the form $B\xi(y)\exp[i(Kx-\Omega t)]$ whose frequency and wavenumber are almost one half those of the fundamental. In this case, B is a constant. When $\epsilon \neq 0$, the presence of the small coefficients, which are periodic in time and streamwise position, leads among other things, to a slow streamwise and time modulation of B. Thus, if the basic wave varies on the scale $x_0 = x$ and $T_0 = t$, the modulation takes place on the scales $x_1 = \epsilon x$, $x_2 = \epsilon^2 x, \ldots$ and $T_1 = \epsilon t$, $T_2 = \epsilon^2 t, \ldots$. Thus, one can use the method of multiple scales[7] and determine an approximate solution to Eqs. (22)–(26). We consider the problem of spatial modulation only for which Ω is exactly one half the fundamental frequency. Moreover, we determine a first-order expansion only and hence need to determine the modulation of the amplitude and the phase of the subharmonic wave on the scale x_1. Hence, we seek a uniform expansion in the form

$$\tilde{u} = u_0(x_0, x_1, y, t) + \epsilon u_1(x_0, x_1, y, t) + O(\epsilon^2), \tag{27}$$

$$\tilde{v} = v_0(x_0, x_1, y, t) + \epsilon v_1(x_0, x_1, y, t) + O(\epsilon^2), \tag{28}$$

$$\tilde{p} = p_0(x_0, x_1, y, t) + \epsilon p_1(x_0, x_1, y, t) + O(\epsilon^2), \tag{29}$$

where $x_1 = \epsilon x$ is a slow scale. Substituting Eqs. (27)–(29) into Eqs. (22)–(26), using Eqs. (11)–(13), and equating coefficients of like powers of ϵ, we obtain

Order ϵ^0:

$$M_1(u_0, v_0) \equiv \frac{\partial u_0}{\partial x_0} + Dv_0 = 0, \tag{30}$$

$$M_2(u_0, v_0, p_0) \equiv \frac{\partial u_0}{\partial t} + U_0\frac{\partial u_0}{\partial x_0} + v_0 DU_0 + \frac{\partial p_0}{\partial x_0} - \frac{1}{R}(D^2 - \frac{\partial^2}{\partial x_0^2})v_0 = 0, \tag{31}$$

$$M_3(u_0, v_0, p_0) \equiv \frac{\partial v_0}{\partial t} + U_0\frac{\partial v_0}{\partial x_0} + Dp_0 - \frac{1}{R}(D^2 - \frac{\partial^2}{\partial x_0^2})v_0 = 0, \tag{32}$$

$$u_0 = v_0 = 0, \quad \text{at } y = 0, \tag{33}$$

$$u_0, v_0 \to 0, \quad \text{as } y \to \infty, \tag{34}$$

Order ϵ:

$$M_1(u_1, v_1) = -\partial u_0/\partial x_1, \tag{35}$$

$$\begin{aligned} M_2(u_1, v_1, p_1) = &- U_0\frac{\partial u_0}{\partial x_1} - [U_1\exp(ikx_0 - i\omega t) + \text{c.c.}]\frac{\partial u_0}{\partial x_0} \\ &- iku_0[U_1\exp(ikx_0 - i\omega t) - \text{c.c.}] \\ &- [V_1\exp(ikx_0 - i\omega t) + \text{c.c.}]Du_0 \\ &- v_0[DU_1\exp(ikx_0 - i\omega t) + \text{c.c.}] \\ &- \frac{\partial p_0}{\partial x_1} + \frac{2}{R}\frac{\partial^2 u_0}{\partial x_0 \partial x_1}, \end{aligned} \tag{36}$$

$$\begin{aligned} M_3(u_1, v_1, p_1) = &- U_0\frac{\partial v_0}{\partial x_1} - [U_1\exp(ikx_0 - i\omega t) + \text{c.c.}]\frac{\partial v_0}{\partial x_0} \\ &- iku_0[V_1\exp(ikx_0 - i\omega t) - \text{c.c.}] \\ &- [V_1\exp(ikx_0 - i\omega t) + \text{c.c.}]Dv_0 \\ &- v_0[DV_1\exp(ikx_0 - i\omega t) + \text{c.c.}] \\ &+ \frac{2}{R}\frac{\partial^2 v_0}{\partial x_0 \partial x_1}, \end{aligned} \tag{37}$$

$$u_1 = v_1 = 0, \quad \text{at } y = 0, \tag{38}$$

$$u_1, v_1 \to 0, \quad \text{as } y \to \infty. \tag{39}$$

III. SOLUTION

A. Basic-state solution

The solutions to Eqs. (14)–(18) can be expressed as

$$U_1 = A\xi_{11}(y), \tag{40}$$

$$V_1 = A\xi_{12}(y), \tag{41}$$

$$p_1 = A\xi_{13}(y), \tag{42}$$

where A is a constant and the $\xi_{1n}(n = 1, 2, 3)$ are the eigenfunctions of the parallel problem given by the following equations:

$$\mathcal{L}_1(\xi_{11}, \xi_{12}; k) = 0, \tag{43}$$

$$\mathcal{L}_2(\xi_{11}, \xi_{12}, \xi_{13}; k, \omega) = 0, \tag{44}$$

$$\mathcal{L}_3(\xi_{11}, \xi_{12}, \xi_{13}; k, \omega) = 0, \tag{45}$$

$$\xi_{11} = \xi_{12} = 0, \quad \text{at } y = 0, \tag{46}$$

$$\xi_{11}, \xi_{12} \to 0, \quad \text{as } y \to \infty. \tag{47}$$

B. Zeroth-order solution

The solution of the zeroth-order problem given by Eqs. (30)–(34) is taken in the form of a Tollmien–Schlichting wave; that is,

$$u_0 = B(x_1)\xi_{21}(y)\exp[i(Kx_0 - \Omega t)] + \text{c.c.}, \tag{48}$$

$$v_0 = B(x_1)\xi_{22}(y)\exp[i(Kx_0 - \Omega t)] + \text{c.c.}, \tag{49}$$

$$p_0 = B(x_1)\xi_{23}(y)\exp[i(Kx_0 - \Omega t)] + \text{c.c.}, \tag{50}$$

The amplitude B is still an undetermined function; it is determined by imposing the solvability condition at the next level of approximation. The quasi-parallel Orr–Sommerfeld problem is

$$\mathcal{L}_1(\xi_{21}, \xi_{22}; K) = 0, \tag{51}$$

$$\mathcal{L}_2(\xi_{21}, \xi_{22}, \xi_{23}; K, \Omega) = 0, \tag{52}$$

$$\mathcal{L}_3(\xi_{21}, \xi_{22}, \xi_{23}; K, \Omega) = 0, \tag{53}$$

$$\xi_{21} = \xi_{22} = 0, \quad \text{at } y = 0, \tag{54}$$

$$\xi_{21}, \xi_{22} \to 0, \quad \text{as } y \to \infty. \tag{55}$$

C. First-order problem

Since the homogeneous parts of Eqs. (35)–(39) are the same as Eqs. (30)–(34) and since the latter equations have a nontrivial solution, the inhomogeneous equations (35)–(39) have a solution if, and only if, a solvability condition is satisfied. The inhomogeneous parts in Eqs. (35)–(39) contain terms proportional to $\exp[ikx_0 - \omega t]$, $\exp[i(kx_0 - \omega t) - i(\bar{K}x_0 - \Omega t]$, their complex conjugates, and others. Secular terms will arise at this order when $k \approx 2K$ and $\omega \approx 2\Omega$; that is, when a subharmonic resonance exists. We consider the case of perfect time resonance and introduce a detuning parameter σ for the spatial part according to

$$k = 2K + \epsilon\sigma, \quad \sigma = O(1), \tag{56}$$

$$\omega = 2\Omega. \tag{57}$$

Using Eqs. (56) and (57), we obtain

$$(kx_0 - \omega t) - (\bar{K}x_0 - \Omega t) = (Kx_0 - \Omega t) + (\sigma x_1 - 2iK_i x_0), \quad (58)$$

where K_i is the imaginary part of K and $\bar{K}$ is the complex conjugate of K.

To determine B, we seek a particular solution for the first-order problem in the form

$$u_1 = z_1(y; x_1)\exp[i(Kx_0 - \Omega t)] + \text{c.c.}, \quad (59)$$

$$v_1 = z_2(y; x_1)\exp[i(Kx_0 - \Omega t)] + \text{c.c.}, \quad (60)$$

$$p_1 = z_3(y; x_1)\exp[i(Kx_0 - \Omega t)] + \text{c.c.} \quad (61)$$

Substituting Eqs. (40)–(42), Eqs. (48)–(50), and Eqs. (56)–(61) into Eqs. (35)–(39) and equating the coefficients of $\exp[i(Kx_0 - \Omega t)]$ on both sides, we obtain

$$\mathcal{L}_1(z_1, z_2; K) = g_1, \quad (62)$$

$$\mathcal{L}_2(z_1, z_2, z_3; K, \Omega) = g_2, \quad (63)$$

$$\mathcal{L}_3(z_1, z_2, z_3; K, \Omega) = g_3, \quad (64)$$

$$z_1 = z_2 = 0, \quad \text{at } y = 0, \quad (65)$$

$$z_1, z_2 \to 0, \quad \text{as } y \to \infty, \quad (66)$$

where g_1, g_2, and g_3 are defined in Appendix A.

To obtain the solvability condition, we multiply Eqs. (62)–(64) by ζ_{21}^*, ζ_{22}^*, and ζ_{23}^*, respectively, where the ζ^*'s are the solutions of the adjoint homogeneous problem, add the equations and integrate the resulting equation by parts from $y = 0$ to $y = \infty$. The adjoint problem corresponding to the eigenvalue K is

$$iK\zeta_{22}^* - D\zeta_{23}^* = 0, \quad (67)$$

$$i(U_0 K - \Omega)\zeta_{23}^* + \zeta_{22}^* DU_0 - D\zeta_{21}^* - R^{-1}(D^2 - K^2)\zeta_{23}^* = 0, \quad (68)$$

$$i(U_0 K - \Omega)\zeta_{22}^* + iK\zeta_{21}^* - R^{-1}(D^2 - K^2)\zeta_{22}^* = 0, \quad (69)$$

$$\zeta_{22}^* = \zeta_{23}^* = 0, \quad \text{at } y = 0, \quad (70)$$

$$\zeta_{21}^*, \zeta_{22}^* \to 0, \quad \text{as } y \to \infty. \quad (71)$$

Then, the solvability condition can be expressed as

$$\int_0^\infty (g_1\zeta_{21}^* + g_2\zeta_{22}^* + g_3\zeta_{23}^*)dy = 0. \quad (72)$$

Substituting for g_1, g_2, and g_3 from Appendix A into Eq. (72), we obtain the following differential equation for the evolution of B

$$\frac{dB}{dx_1} = \frac{f_2}{f_1} A\bar{B}\exp(i\sigma x_1 - 2K_i x_0), \quad (73)$$

where f_1 and f_2 are given in quadratures in terms of ζ_{2n}, ζ_{2n}^*, k, and K and they are defined in Appendix B. In terms of the original variable x, Eq. (73) can be rewritten as

$$\frac{dB}{dx} = \epsilon\frac{f_2}{f_1} A\bar{B}\exp[i(k - 2K_r)x], \quad (74)$$

where K_r is the real part of K.

IV. EFFECT OF BOUNDARY-LAYER GROWTH

The analysis presented in the preceding section did not account for the growth of the mean boundary layer. If $\epsilon_1 \gg \epsilon$, the effect of the fundamental on the subharmonic is negligible compared with the effect of the boundary-layer growth. In this case, Eq. (74) is replaced by

$$\frac{dB}{dx} = \epsilon_1 \frac{f_3}{f_1} B, \quad (75)$$

where f_3 is defined in Appendix B. If $\epsilon_1 = O(\epsilon)$, carrying out an analysis similar to that in the preceding two sections yields

$$\frac{dB}{dx} = \epsilon_1 \frac{f_3}{f_1} B + \epsilon \frac{f_2}{f_1} A\bar{B}\exp[i\int (k - 2K_r)dx]. \quad (76)$$

We note that the algebra involved in deriving Eq. (76) is much more involved than that needed to derive either Eq. (74) or Eq. (75). One can easily verify that Eq. (76) tends to Eq. (74) when $\epsilon \gg \epsilon_1$ and it tends to Eq. (75) when $\epsilon \ll \epsilon_1$.

It is convenient to introduce the transformation

$$a = A\exp(-\int K_i dx), \quad b = B\exp(-\int K_i dx), \quad (77)$$

so that a and b account for the quasi-parallel growth rates of the fundamental and its subharmonic. Then, Eq. (76) can be rewritten as

$$\frac{db}{dx} = (\epsilon_1 \frac{f_3}{f_1} - K_i)b + \epsilon \frac{f_2}{f_1} a\bar{b}\exp(i\theta), \quad (78)$$

where

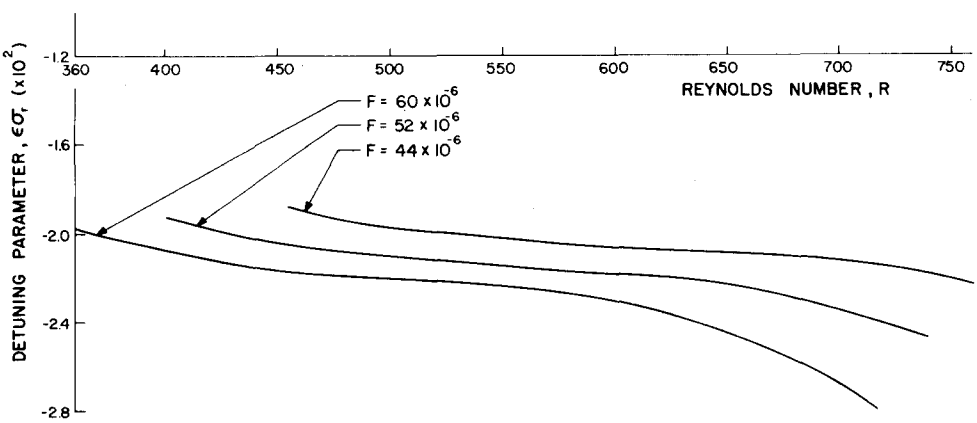

FIG. 1. Detuning parameter, $\epsilon\sigma_r$.

$$\frac{d\theta}{dx} = \epsilon\sigma_r = \mathrm{Re}(k - 2K) . \tag{79}$$

Since the variations of the real parts of k and K with streamwise position are very small, the variation of σ_r with R is also very small as shown in Fig. 1.

Since K_i (imaginary part of K) and a (amplitude of the fundamental) are functions of the streamwise position, we were unable to determine an exact solution for Eq. (78). However, a qualitative description of the stability characteristics can be obtained by analyzing the local solutions of Eq. (78) presented in Sec. VI.

V. COMPUTATIONAL PROCEDURE

A. Solutions of the basic-state and the zeroth-order problems

The procedure for the solutions of the basic state and the zeroth-order problem, given by Eqs. (43)–(47) and Eqs. (51)–(55), respectively, are the same; therefore, we will explain the methodology only for the basic-state problem.

Equations (43)–(47) can be expressed as a system of first-order differential equations; that is,

$$dz/dy = Gz , \tag{80}$$

where z is a 4×1 matrix with the elements

$$z_1 = \zeta_{11}(y), \quad z_2 = D\zeta_{11}(y), \quad z_3 = \zeta_{12}(y), \quad z_4 = \zeta_{13}(y) , \tag{81}$$

and the elements of the 4×4 G matrix are given in Appendix C.

To determine starting solutions for the integration of Eqs. (80), we assume that $U_0 = 1$, $DU_0 = 0$, and $D^2U_0 = 0$ at $y = y_0$ with y_0 being any value of y larger than the boundary layer thickness. The matrix G then has constant coefficients at $y = y_0$ and Eqs. (80) have solutions of the form

$$z_i = \sum_{j=1}^{4} c_{ij}\exp(\lambda_j y) \text{ for } i = 1,2,3,4 , \tag{82}$$

where the c_{ij} are constants, the λ's are the solutions of

$$|G - \lambda I| = 0 , \tag{83}$$

and I is the identity matrix. Equation (83) has the roots

$$\lambda_{1,2} = \pm k, \quad \lambda_{3,4} = \pm[k^2 + i(k - \omega)R]^{1/2} . \tag{84}$$

Two of these roots have positive real parts and make the solution grow exponentially as $y \to \infty$ and must be discarded according to the boundary conditions. This leaves two linear independent solutions that decay exponentially with y.

The eigenvalues are not known *a priori* and must be determined along with the eigenfunctions. For given values of ω and R, we guess a value for k, and integrate the system of equations from $y = y_0$ to $y = 0$. If the guessed value of k does not satisfy the boundary conditions at $y = 0$, k is incremented by using a Newton-Raphson scheme and the procedure is repeated until the boundary conditions are satisfied. Integration is done by using a technique developed by Scott and Watts.[11] This technique orthonormalizes the solution of the set of equations whenever a loss of independence is detected.

B. Solution of the adjoint problem

The solution procedure is exactly the same as for the solution of the basic-state problem. The coefficients of the z matrix are

$$z_1 = \zeta_{22}^*(y), \quad z_2 = D\zeta_{22}^*(y), \quad z_3 = \zeta_{23}^*(y), \quad z_4 = \zeta_{21}^*(y) , \tag{85}$$

and the adjoint problem has the same eigenvalues as the zeroth-order problem.

C. Solution of Eqs. (78) and (79)

The calculations are repeated at different x locations to evaluate f_1, f_2, f_3, k, and K for a given frequency along the x axis. A fourth-order fixed step size Runge–Kutta integration scheme is used to solve Eqs. (78) and (79) to find the amplitude of the subharmonic mode for different initial amplitudes of the fundamental mode.

VI. NUMERICAL RESULTS AND CONCLUDING REMARKS

Computations were performed for three different dimensionless frequencies of the subharmonic wave, $F = 60\times10^{-6}$, 52×10^{-6}, and 44×10^{-6}, by using different values of ϵ, where $F = \Omega/R = \Omega^*\nu/U_\infty^2$ with Ω being the dimensionless boundary-layer frequency and Ω^* being the dimensional angular frequency of the subharmonic wave. In all the numerical calculations presented here, ϵ is taken to be the initial amplitude of the fundamental wave as a fraction of the mean flow. For a growing boundary layer, a is not a constant and it is calculated by using Eqs. (5) and (77) subject to the normalized initial condition of unity. All calculations are started at a location near the first neutral stability point of the fundamental wave and continued farther downstream well into the unstable region of the subharmonic mode. The variations of a with R (i.e., streamwise position) are shown in Fig. 2. We note from Fig. 1 that the detuning parameter $\epsilon\sigma_r$ is a weakly varying function of streamwise position. Nevertheless, it is calculated at each streamwise position from the calculated values of k and K. Then, θ is calculated from Eq. (79). The function $b(x)$ is normalized to unity at the starting point.

As discussed in Sec. IV, we were unable to determine a closed-form solution to Eq. (78); therefore, we numerically integrated this equation. However, before presenting these numerical results, we investigate the quasi-stationary solutions of Eq. (78). To this end, we neglect the nonparallel growth rate $\epsilon_1 f_3/f_1$ and consider K_i, f_2/f_1, ϵa, and $\epsilon\sigma_r$ to be constant. Thus, we rewrite Eq. (78) as

$$db/dx = -K_i b + \Lambda\bar{b}\exp(i\sigma_r x + i\phi) , \tag{86}$$

where

$$\Lambda = \epsilon|f_2 f_1^{-1}|a, \quad \phi = \mathrm{Im}[\log(f_2 f_1^{-1})] . \tag{87}$$

It is convenient to introduce the transformation

$$b = (g_r + ig_i)\exp[\tfrac{1}{2}i(\sigma_r x + \phi)] \tag{88}$$

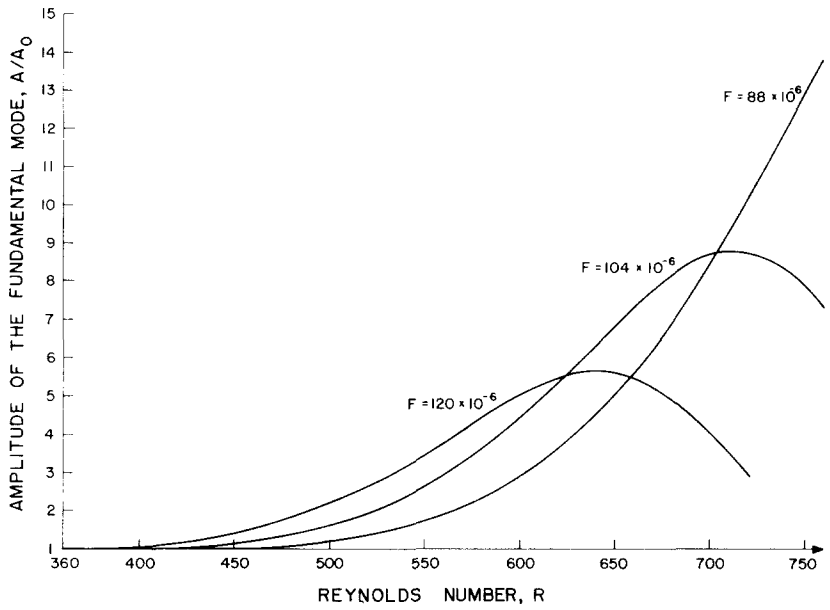

FIG. 2. Amplitude of the fundamental mode at different frequencies.

in Eq. (86), where g_r and g_i are real. Then, separating real and imaginary parts yields

$$dg_r/dx + (K_i - \Lambda)g_r - \tfrac{1}{2}\epsilon\sigma_r g_i = 0\,, \tag{89}$$

$$dg_i/dx + (K_i + \Lambda)g_i + \tfrac{1}{2}\epsilon\sigma_r g_r = 0\,. \tag{90}$$

Equations (89) and (90) admit solutions of the form

$$g_r = c_1\exp(\lambda x), g_i = c_2\exp(\lambda x)\,, \tag{91}$$

where c_1 and c_2 are constants and

$$\lambda = -K_i \pm (\Lambda^2 - \tfrac{1}{4}\epsilon^2\sigma_r^2)^{1/2}\,. \tag{92}$$

Since $-K_i$ is the linear spatial growth rate of the subharmonic, Eqs. (88), (91), and (92) show that the parametric resonance (i.e., effect of fundamental wave on its subharmonic) is destabilizing when

$$\Lambda^2 > \tfrac{1}{4}\epsilon^2\sigma_r^2\,. \tag{93}$$

Using Eq. (87), we rewrite this condition as

$$\epsilon a > \tfrac{1}{2}\epsilon\,|\sigma_r f_1/f_2|\,. \tag{94}$$

We note from Figs. 1 and 3 that, for a given frequency, $\epsilon|\sigma_r|$ and $|f_1/f_2|$ are almost constant functions of R. Therefore, Eq. (94) defines, for each frequency, an approximate critical value of the amplitude ϵa of the fundamental wave to trigger the parametric resonance instability. It follows from Figs. 1 and 2 and Eq. (94) that the critical amplitude is approximately 29% of the mean flow for these frequencies.

Figures 4, 5, and 6 show the results obtained from the numerical integration of Eq. (78). They illustrate the variation of $b(x)$ with R and ϵ. The solid curves are for the case of no interaction between the fundamental wave and its subharmonic. The point where the solid curve has a minimum is the first neutral stability point of the subharmonic mode.

Figure 4 shows that, when $\epsilon a = 0.02$ or 0.04, the amplitude function $b(x)$ for $F = 60\times10^{-6}$ oscillates around the solid curve (i.e., its value in the absence of interaction). Calculating the local values of ϵa from Fig. 2 and the fact that $\epsilon a = (\epsilon a_0)(a/a_0)$, we see that ϵa does not attain the critical amplitude of 29% predicted by the quasi-stationary solution for these initial amplitudes. However, when $\epsilon a_0 = 0.06$, it follows from Fig. 2 that ϵa reaches the critical value needed to trigger the parametric instability at $R \approx 590$. This is verified in Fig. 4 which shows that b oscillates around the solid curve ahead of $R \approx 590$ and increases

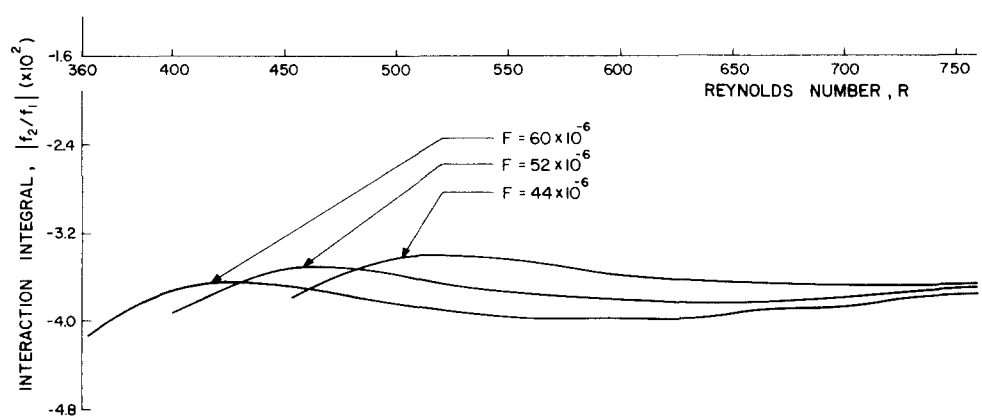

FIG. 3. Interaction integral, $|f_2/f_1|$.

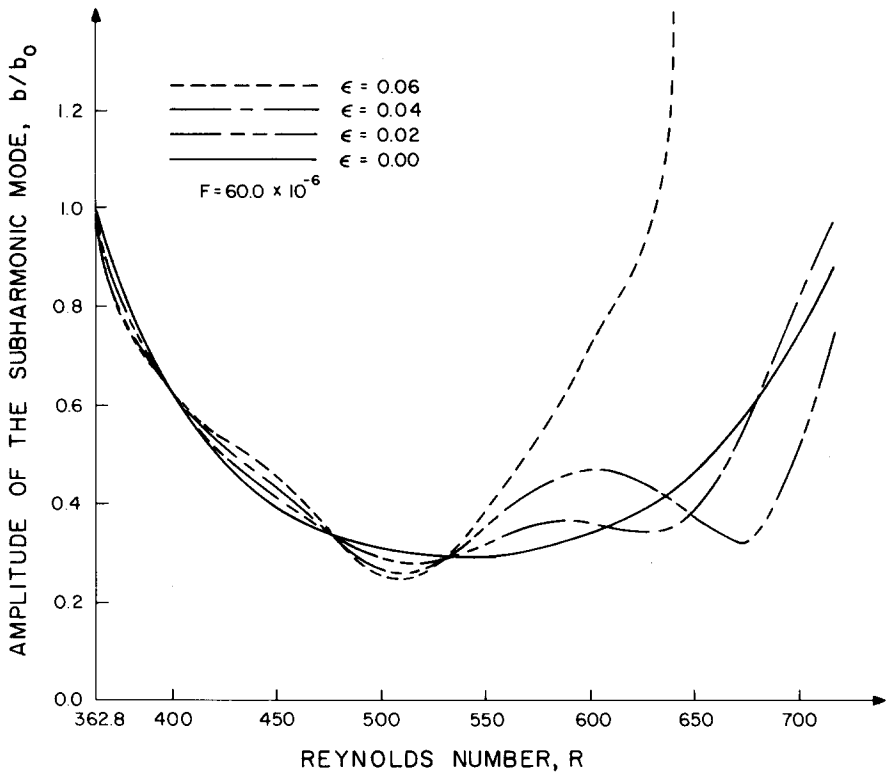

FIG. 4. Amplitude of the subharmonic mode at $F = 60 \times 10^{-6}$ for different initial amplitudes of the fundamental mode.

sharply downstream of $R \approx 590$.

When $F = 52 \times 10^{-6}$ and $\epsilon a_0 = 0.02$, it follows from Fig. 2 that the critical value of ϵa is never reached and hence, according to the quasi-stationary solution, b is expected to oscillate around its noninteraction value. This is verified by the numerical solution shown in Fig. 5. When $\epsilon a_0 = 0.04$, Fig. 2 shows that ϵa reaches the critical amplitude at $R \approx 670$. Hence, b is expected to oscillate around its noninteraction value ahead of $R \approx 670$ and increase sharply downstream of $R \approx 670$. Again, this conclusion is verified by the numerical solution shown in Fig. 5. If ϵa_0 is increased further, the critical amplitude will be reached at a farther upstream

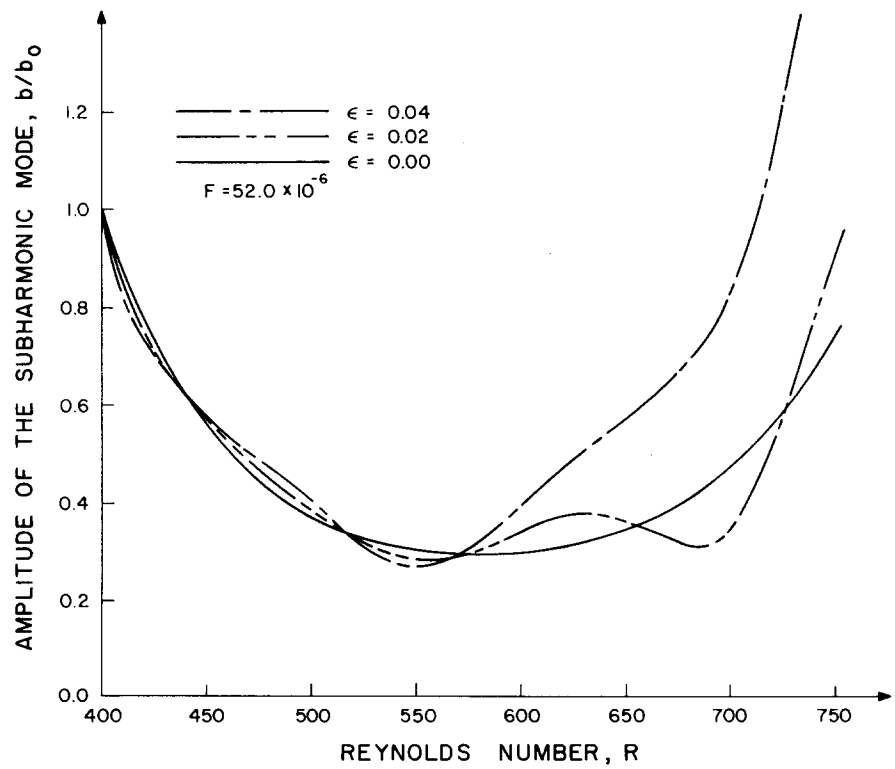

FIG. 5. Amplitude of the subharmonic mode at $F = 52 \times 10^{-6}$ for different initial amplitudes of the fundamental mode.

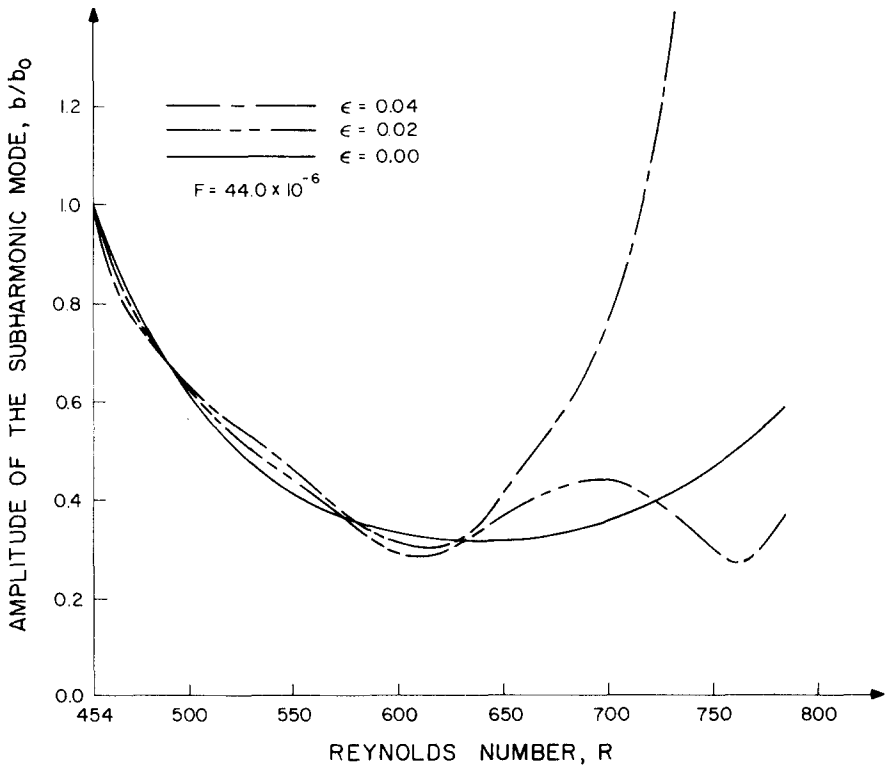

FIG. 6. Amplitude of the subharmonic mode at $F=44\times10^{-6}$ for different initial amplitudes of the fundamental mode.

location.

When $F=44\times10^{-6}$, Fig. 6 shows that b oscillates around its noninteraction value if $\epsilon a_0=0.02$, while it increases sharply downstream of $R\approx685$ if $\epsilon a_0=0.04$. These numerical results corroborate the predictions of the quasi-stationary solution because Fig. 2 shows that ϵa does not reach the critical value if $\epsilon a_0=0.02$, while it reaches the critical value at $R\approx685$ if $\epsilon a_0=0.04$.

The large amplitude 0.29 of the fundamental wave needed to trigger the parametric instability in the Blasius flow is a consequence of the large detuning parameter $\epsilon\sigma_r$ according to Eq. (94). For flows in which $\epsilon\sigma_r$ is small such as the free-shear layer flow,[6,12] the critical amplitude will be small, and the parametric instability will be triggered with smaller amplitudes of the fundamental wave. We should note that many other nonlinear effects take place before the parametric instability is triggered in the flow over a flat plate. In fact, the flow will become turbulent before ϵa reaches the critical value for parametric instability. Thus, the observed subharmonics in the experiments of Refs. 2 and 3 are not the consequence of the parametric instability discussed here. In the parametric instability model, the amplitude of the subharmonic is infinitesimal and hence it does not affect the fundamental wave. Some preliminary calculations using a nonlinear interaction mode between a fundamental wave and its subharmonic indicate that both waves can be greatly destabilized if the initial amplitude of the subharmonic wave is not infinitesimal. This would be possible if the disturbance created by a vibrating ribbon contains the fundamental frequency and its subharmonic. This conclusion has been supported by recent experiments of Saric and Reynolds.[13]

ACKNOWLEDGMENTS

The authors are indebted to Dr. W. S. Saric for many helpful discussions and comments.

This work was supported by the United States Office of Naval Research Contract No. NR 061-201 and the National Aeronautics and Space Administration's Langley Research Center Grant No. NSG 1255.

APPENDIX A

$$g_1=-\frac{dB}{dx_1}\zeta_{21}\,, \tag{A1}$$

$$g_2=-U_0\frac{dB}{dx_1}\zeta_{21}-\frac{dB}{dx_1}\zeta_{23}+\frac{2iK}{R}\frac{dB}{dx_1}\zeta_{21} -[i(k-\bar{K})\zeta_{11}\bar{\zeta}_{21}+\zeta_{12}D\bar{\zeta}_{21} +D\zeta_{11}\bar{\zeta}_{22}]A\bar{B}\exp(i\sigma x_1-2K_i x_0)\,, \tag{A2}$$

$$g_3=-U_0\frac{dB}{dx_1}\zeta_{22}+\frac{2iK}{R}\frac{dB}{dx_1}\zeta_{22}-[-\bar{K}\zeta_{11}\bar{\zeta}_{22}+ik\zeta_{12}\bar{\zeta}_{21} +\zeta_{12}D\bar{\zeta}_{22}+D\zeta_{12}\bar{\zeta}_{22}]A\bar{B}\exp(i\sigma x_1-2K_i x_0)\,. \tag{A3}$$

APPENDIX B

$$f_1=\int_0^\infty[-\zeta_{21}\zeta_{21}^*-(U_0\zeta_{21}+\zeta_{23})\zeta_{22}^*-U_0\zeta_{22}\zeta_{23}^* +(2iK/R)(\zeta_{21}\zeta_{22}^*+\zeta_{22}\zeta_{23}^*)]dy\,, \tag{B1}$$

$$f_2=\int_0^\infty[i(k-\bar{K})\zeta_{11}\bar{\zeta}_{21}+\zeta_{12}D\bar{\zeta}_{21}+D\zeta_{11}\bar{\zeta}_{22}]\zeta_{22}^* +[-i\bar{K}\zeta_{11}\bar{\zeta}_{22}+ik\zeta_{12}\bar{\zeta}_{21}+\zeta_{12}D\bar{\zeta}_{22}+D\zeta_{12}\bar{\zeta}_{22}]\zeta_{23}^*dy\,, \tag{B2}$$

$$f_3=\int_0^\infty\Bigg[\frac{\partial\zeta_{21}}{\partial\tilde{x}_1}\zeta_{21}^*+\zeta_{22}^*\Big(U_0\frac{\partial\zeta_{21}}{\partial\tilde{x}_1}+\frac{\partial U_0}{\partial\tilde{x}_1}\zeta_{21}$$

$$+V_0D\zeta_{21}+\frac{\partial\zeta_{23}}{\partial\tilde{x}_1}\Big)+\Big(U_0\frac{\partial\zeta_{22}}{\partial\tilde{x}_1}+V_0D\zeta_{22}+\zeta_{22}DV_0\Big)\zeta_{23}^*$$

$$-\frac{2iK}{R}\Big(\frac{\partial\zeta_{21}}{\partial\tilde{x}_1}\zeta_{22}^*+\frac{\partial\zeta_{22}}{\partial\tilde{x}_1}\zeta_{23}^*\Big)$$

$$-\frac{2i}{R}\frac{dK}{d\tilde{x}_1}(\zeta_{21}\zeta_{22}^*+\zeta_{22}\zeta_{23}^*)\Bigg]dy\,, \tag{B3}$$

where $\tilde{x}_1=\epsilon_1 x$ and $\epsilon_1=R^{-1}$ expressing the slight nonparallelism of the flow.

APPENDIX C

$$g_{11}=0,\quad g_{12}=1,\quad g_{13}=0,\quad g_{14}=0, \tag{C1}$$

$$g_{21}=i(U_0k-\omega)R+k^2,\quad g_{22}=0,$$

$$g_{23}=R(dU_0/\partial y),\quad g_{24}=ikR, \tag{C2}$$

$$g_{31}=-ik,\quad g_{32}=g_{33}=g_{34}=0, \tag{C3}$$

$$g_{41}=0,\quad g_{42}=-ik/R,$$

$$g_{43}=-[i(U_0k-\omega)+k^2/R],\quad g_{44}=0. \tag{C4}$$

[1]P. S. Klebanoff, K. D. Tidstrom, and L. M. Sargent, J. Fluid Mech. **12**, 1 (1962).
[2]I. S. Kachanov, V. V. Kozlov, and V. Levchenko, Mek. Zhid. Gaza **3**, 4 (1977).
[3]E. V. Veasov, A. S. Ginevsky, and R. K. Karavosov, in *Turbulent Flows*, edited by V. V. Struminskii (Nauka, Moscow, 1977), p. 90.
[4]H. Sato, J., Phys. Soc. Jpn. **14**, 1797 (1959).
[5]R. Wille, Air Force Office of Scientific Research Report 61 (052)-412 (1963).
[6]R. E. Kelly, J. Fluid Mech. **27**, 4 (1967).
[7]A. H. Nayfeh, *Perturbation Methods* (Wiley, New York, 1973), Chap. 6.
[8]A. H. Nayfeh, W. S. Saric, and D. T. Mook, Arch. Mech. Stosow **26**, 401 (1974).
[9]W. S. Saric and A. H. Nayfeh, Phys. Fluids **18**, 945 (1975).
[10]C. von Kerczek, in *Proceedings of the Twelfth Symposium on Naval Hydrodynamics* (National Academy of Sciences, Washington, D. C., 1979) (to be published).
[11]M. R. Scott and H. Watts, SIAM J. Numer. Anal. **14**, 40 (1977).
[12]A. Michalke, J. Fluid Mech. **19**, 543 (1964).
[13]W. S. Saric and G. Reynolds, Bull. Am. Phys. Soc. **23**, 8 (1978).